ICSV13 - Vienna
The Thirteenth International Congress on Sound and Vibration
Vienna, Austria, July 2-6, 2006

COMPUTATION OF COMPLEX DYNAMIC STIFFNESS OF INFLATED DIAPHRAGM IN PNEUMATIC SPRINGS BY USING FE CODES

Jeung-Hoon Lee* and Kwang-Joon Kim

Center for Noise and Vibration Control, Department of Mechanical Engineering, KAIST
Science Town, Daejeon 305-701, South Korea
olo@kaist.ac.kr

Abstract

Accurate modeling of complex dynamic stiffness of the pneumatic springs is crucial for an efficient design of vibration isolation tables for precision instruments such as optical devices or nano-technology equipments. Besides pressurized air itself, diaphragm made of rubber materials, essentially employed for prevention of air leakage, plays a significant contribution to the total complex stiffness. Therefore, effects of the diaphragm should be taken care of precisely. The complex stiffness of an inflated diaphragm is difficult to predict or measure, since it is always working together with the pressurized air. In our earlier research, the complex stiffness of a diaphragm was indirectly estimated simply by subtracting stiffness of the pressurized air from measurement of the total complex stiffness for a single chamber pneumatic spring. In order to reflect dynamic stiffness of inflated diaphragm on the total stiffness at the initial design or design improvement stage, however, it is required to be able to predict beforehand. In this presentation, how to predict the complex stiffness of inflated rubber diaphragm by commercial FE codes(e.g. ABAQUS) will be discussed and the results will be compared with the indirectly measured values.

INTRODUCTION

Often, the vibration environments for precision instruments such as optical devices, nano-scale equipments, etc, are complied with pneumatic springs, which have lower stiffness than that of conventional rubber or coil springs. As the vibration regulations for precision instruments[1,2] become more stringent, it is required for the pneumatic springs to have better isolation performance, which could be efficiently done by design improvement. For this purpose, first of all, an accurate complex stiffness model of the pneumatic springs would be needed.

A schematic diagram of a pneumatic spring is shown in Figure 1, where a piston

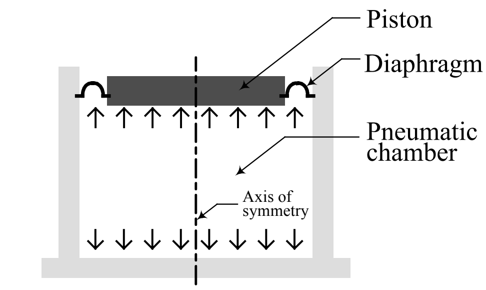

Figure.1 Schematics of pneumatic spring

and a diaphragm enclose pressurized air inside a chamber. The rigid piston supports payload mass consisting an isolation table and/or a precision instrument on it. The diaphragm, a rubber membrane of complicated shape is installed for prevention of air leakage. Thus, the air in the pneumatic chamber eventually works together with the diaphragm as a stiffness element, when the vibrations of base or payload cause the compression/expansion of the air.

Harris et. al.[3] and DeBra[4] proposed a model for pneumatic spring by describing just the stiffness characteristic of the air in the chamber, which was done by consideration of thermo-dynamic relationship. But a practical pneumatic spring shows not only a higher stiffness value but also a higher damping characteristics than the model of the air inside the pneumatic chamber[5]. In other words, the stiffness of the air only cannot represent the actual behaviour of the pneumatic spring fully, which may be due to effects of the diaphragm. As the diaphragm expands by the pressurized air, it plays indeed the role of another complex stiffness element in the pneumatic springs. Hence it is very natural to include the complex stiffness of the diaphragm in the model of pneumatic springs. But it would not be easy to model accurately the diaphragm in an analytical way because it is a rubber membrane of complicated shape. Furthermore, the complex stiffness of diaphragm alone cannot be measured directly, because it is expandable only by pressurization of air inside the chamber as mentioned previously.

In our earlier research[6], the complex stiffness of a diaphragm was indirectly estimated simply by subtracting stiffness of the pressurized air from measurement of the total complex stiffness for a single chamber pneumatic spring. Estimated results provided here exhibited quite a good match to the typical characteristics of viscoelastic material, which mainly constitutes diaphragm. Hence, it was believed that major portion of estimated results come from the complex stiffness of the diaphragm. But, there was an argument that the results might contain effects of unknown dynamics besides the diaphragm. This motivates us to validate the indirectly estimated results by a computational way using FEM. Furthermore, to facilitate the initial design or design improvement stage of pneumatic spring, it is previously required to be able to predict the complex stiffness of inflated diaphragm. Thus this paper will cover how to compute the complex stiffness of inflated diaphragm by commercial FE codes(e.g. ABAQUS). Then, comparison to the indirectly estimated results will be given subsequently.

CALCULATION OF DIAPHRAGM COMPLEX STIFFNESS BY FEM

In this study, two stages of both nonlinear static- and linear dynamic- FE analysis were employed for calculations of the diaphragm complex stiffness. The objective of nonlinear static analysis is just to obtain equilibrium configuration of inflated diaphragm after pressurization. In the linear dynamic analysis, then, the inflated diaphragm under static equilibrium was sinusoidally excited to calculate its complex stiffness.

Nonlinear static analysis

Figure 2. Full view of diaphragm

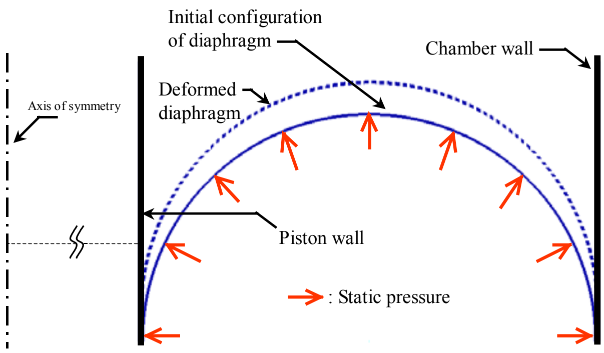

Figure 3. FE model of diaphragm

Since the diaphragm in Figure 2 experiences a large deformation(extention) during the inflation by static pressure, nonlinear static analysis is required. To do this end, cross section of diaphragm was assumed to be a semicircle, then a FE model shown in Figure 3 was firstly constructed by using one dimensional axi-symmetric elements(CAX4H,[7]) based on Mooney-Rivlin theory. Below, the constitutive equation of Mooney-Rivlin model[8] that can represent well the nonlinear static behaviour is presented. In a uni-axial uniform deformation, the stress σ is expressed by

$$\sigma=2(C_1\lambda+C_2)\left(\lambda-\frac{1}{\lambda^2}\right) \tag{1}$$

where the extensional stretch $\lambda(=1+\varepsilon)$ is related to the engineering strain ε. In equation (1), the coefficients C_1 and C_2 are constants to be determined from the static test data.

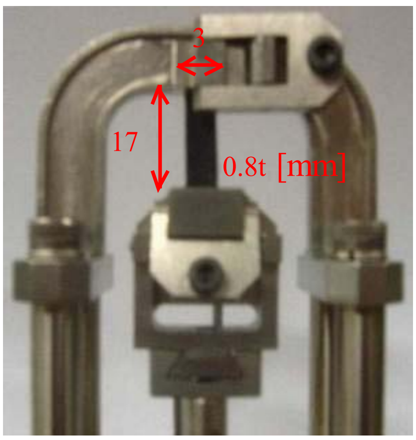

Figure.4 Experimental setup for the static tension test

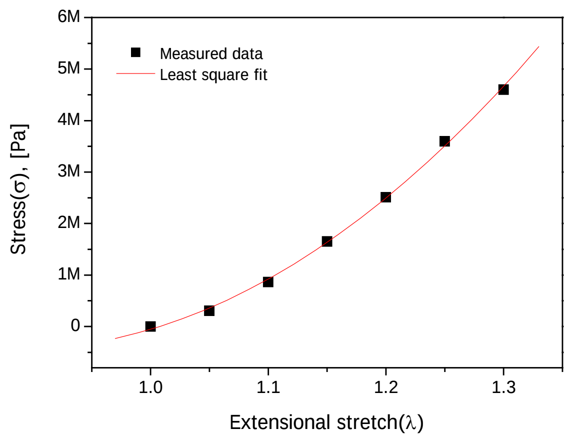

Figure.5 Experimental results of static tension test

Figure 4 shows a measurement set-up for the static test, where the specimen (Length:17mm, Width:3mm, Thickness:0.8mm) was installed in material testing system (model:DMA2980, TA instrument) driven via computer controlled servo-electric motor actuation systems. The specimen was stretched by 5~30%, i.e. λ=1.05 ~1.3, and stress measurements for each stretch were made after 20 minutes relaxation. Square boxes in Figure 5 represent measurement results that determine the values of C_1 and C_2. The least square fit with Equation (1), when C_1 and C_2 have 8.7 and -0.8 [MPa] respectively, is shown as solid line in Figure 5. Now, applying a static pressure to the FE model of diaphragm can give deformed(inflated) configuration of diaphragm, as dotted line in Figure 3.

Linear dynamic analysis

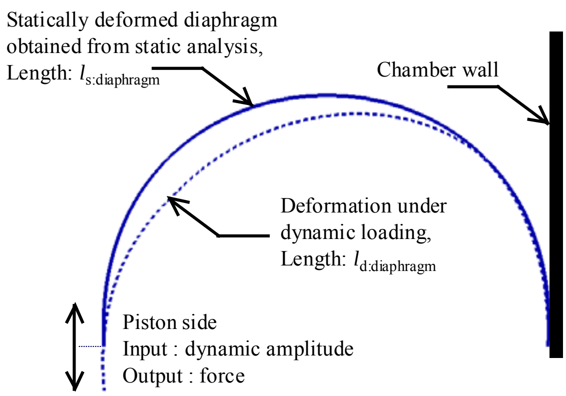

Figure.6 Linear dynamic analysis

In dynamic analysis, sinusoidal displacement excitations are applied to the piston side of statically deformed diaphragm obtained from static analysis, while calculating the output force at that point as depicted in Figure 6. It should be emphasized that static pressure used in prior analysis must be excluded to reject the transmitted force to piston caused by pressure. In addition, the complex modulus of typical rubber material depends on an amplitude of dynamic strain as well as pre-strain[8]. Therefore, characterization of complex modulus subject to pre-strain ε_0, which corresponds to pressure induced static deformation, should be conducted in dynamic analysis stage. In this study, the following scheme was used to determine the pre-strain ε_0 in dynamic characterization

$$\varepsilon_0 = \frac{l_{s:diaphragm} - l_{0:diaphragm}}{l_{0:diaphragm}} \tag{2}$$

where $l_{s:diaphragm}$ and $l_{0:diaphragm}$ are both deformed- and initial- length of diaphragm. In the same manner, input dynamic strains ε_d for dynamic characterization can be resolved as follows.

$$\varepsilon_d = \frac{l_{d:diaphragm} - l_{s:diaphragm}}{l_{s:diaphragm}} \tag{3}$$

$l_{d:diaphragm}$ in the above denotes the deformed length of diaphragm under dynamic loading as expressed in Figure 6. But a bottleneck is that $l_{d:diaphragm}$ cannot be known without complex modulus data to be measured. In order to obtain approximate value of $l_{d:diaphragm}$, secondary static analysis applying the dynamic displacement amplitude at the piston side was performed. Table 1 summarizes the dynamic displacement amplitude at the piston X_p used in the secondary static analysis and the resulting ε_d for the dynamic characterization of specimen.

Table.1 Summary of X_p and ε_d

X_p [mm]	0.05	0.07	0.09	0.15	0.30	0.50
ε_d	1.3×10^{-5}	1.8×10^{-5}	2.4×10^{-5}	4.0×10^{-5}	8.1×10^{-5}	14.1×10^{-5}

By using the values of ε_d superimposed on pre-strain ε_0(11%) of the specimen, measurements of the complex modulus between 0.2 and 25Hz were made, as represented in Figure 7. These complex modulus data were applied to the complex stiffness calculation of inflated diaphragm. For reference, different complex modulus data, which were obtained by the consideration of static-strain distribution in the diaphragm, need to be employed for each element of FE model. That may improve the quality of FE results, since the static-strain distributions of diaphragm are not uniform. But it is tedious and time-consuming works in state of the art of commercial FE codes. There was a systematic approach[9] that assigns complex modulus data by element. However, this technique will not be tried throughout this paper, while assigning a single complex modulus data for the whole elements.

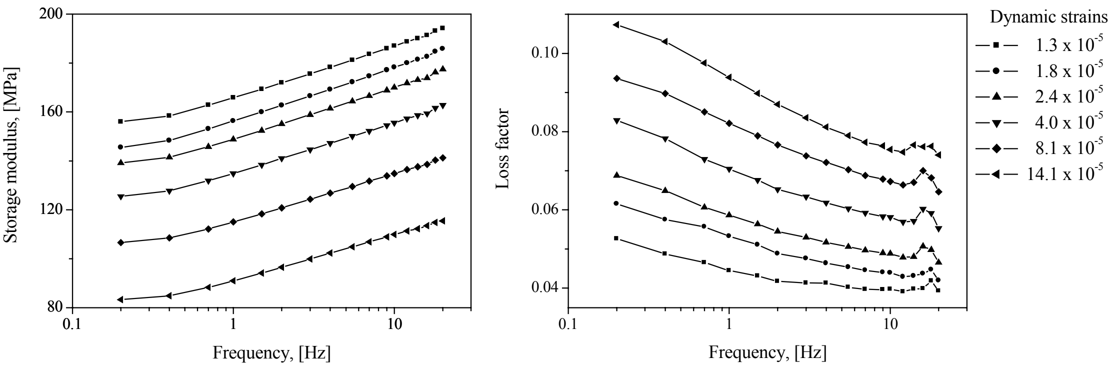

Figure.7 Measured complex modulus E^*, ε_0=11%; Storage modulus : Re[E^*], loss factor : Im[E^*]/Re[E^*]

INDIRECT ESTIMATION OF COMPLEX STIFFNESS OF DIAPHRAGM

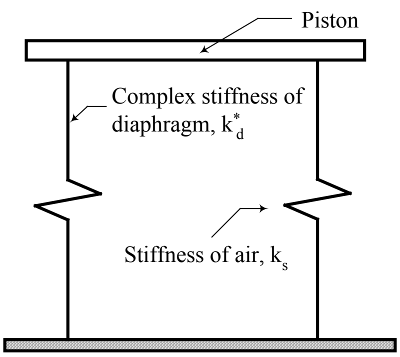

Figure.8 Equivalent mechanical model of pneumatic spring

As mentioned in the introduction, the diaphragm will deform together with the pressure change inside the chamber. That is, measurements of the complex stiffness of the pneumatic spring contain effects of both air in the chamber and diaphragm in parallel as shown in Figure 8. Therefore, the complex stiffness of diaphragm can be obtained by simply subtracting the theoretical air stiffness k_s from measurements of the pneumatic spring as follows.

$$k_d^*(X_p, \omega) = k_{exp}^*(X_p, \omega) - k_s \tag{4}$$

where, $k^*_{exp}(X_p,\omega)$ in Equation (4) denotes the experimentally measured complex stiffness of the pneumatic spring, which may have a frequency ω and dynamic amplitude X_p dependent characteristics. The stiffness of air k_s, which is essential for the extraction of the complex stiffness of diaphragm, is shown in Equation (5). Full derivation of k_s requires consideration of both the first law of thermodynamics and the ideal gas law in pneumatic chamber. Details can be found in reference[6].

$$k_s = \frac{\kappa p_0 A_p^2}{V_0} \tag{5}$$

κ(=1.4) in the above denotes the specific heat ratio. And p_0 and V_0 designate supplied pressure and chamber volume, respectively, both of which are obtainable from direct measurements. Finally, A_p represents the equivalent piston cross-sectional area under the assumption that the dynamic behavior of the piston and the diaphragm can be represented by that of a single piston. Using the described variables above and Equations (4), (5), the complex stiffness of diaphragm can be measured indirectly.

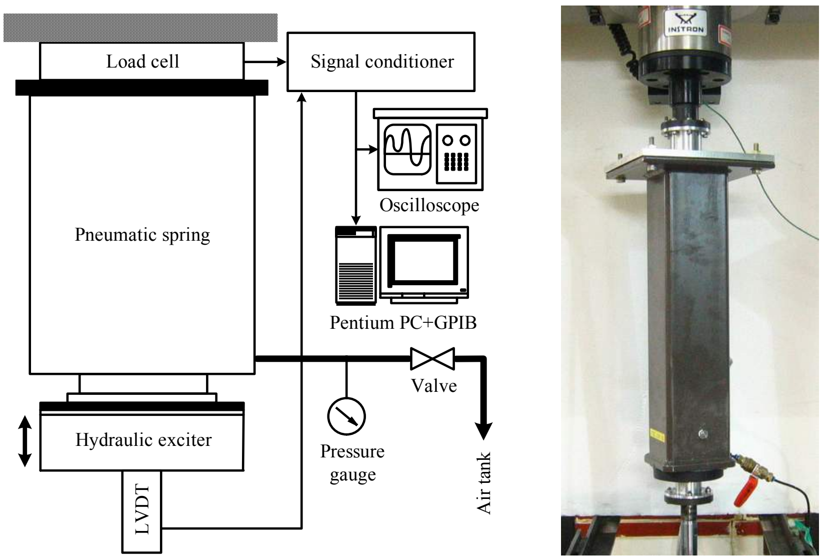

Figure.9 Experimental setup for the measurements of the complex stiffness of pneumatic spring k^*_{exp}

Table.2 Design specifications of employed pneumatic spring for experiments

Symbol	Name	Value	
κ	Specific heat ratio of air	1.4	
p_0	Supplied pressure	4.93×10^5	[Pa]
V_0	Chamber volume	8.1×10^{-4}	[m^3]
A_p	Effective piston area	5.3×10^{-3}	[m^2]
$k_s(=\kappa p_0 A_p^2/V_0)$	Stiffness of air	23	[kN/m]

An experimental apparatus to apply the indirect measurement method explained above is shown in Figure 9. The pneumatic spring(Specifications are in Table 2.) with the applied pressure p_0 was installed in the INSTRON dynamic material testing system(model:8502) driven via computer controlled servo-hydraulic actuation systems. The displacement and the force signals were measured by LVDT(Linear Variable

Differential Transformer) and load cell respectively. The measured signals were post-processed to obtain the complex stiffness. The thick line in Figure 9 represents the pneumatic transmission line, and a pressure gauge was installed to measure the applied pressure in the chamber, i.e. the pressure at static equilibrium, p_0. Various sinusoidal displacement excitations, all of which are the same as the conditions of material characterization(Listed in Table 1), were applied to the piston under a given preload corresponding to the weight of a payload mass(100kg).

The measured complex stiffness of inflated diaphragm obtained by equation (4) is shown as solid lines in Figure 10. Real part and loss factor are related to the stiffness and damping characteristics, respectively. First of all, it is interesting to note that measured complex stiffness of diaphragm exhibits a frequency- and dynamic amplitude- dependent behavior. More precisely, the real part representing the elastic stiffness increases with frequency and decreases with dynamic amplitude, showing the behavior of a softening spring. Frequency dependence of the loss factor is not as significant as that of the stiffness while the loss factor increases with the dynamic amplitude. Those observed behaviors for the complex stiffness of inflated diaphragm nearly resembles to typical characteristics of viscoelastic materials[8]. From the above observations, it is reasonable to regard that the indirectly estimated complex stiffness is due to the one of diaphragm, mainly consisting of viscoelastic materials. But, the indirectly estimated results may contain effects of unknown dynamics besides the diaphragm, such as nonlinearity of the air due to compressibility. Hence, these experimental data need to be compared to the calculated ones.

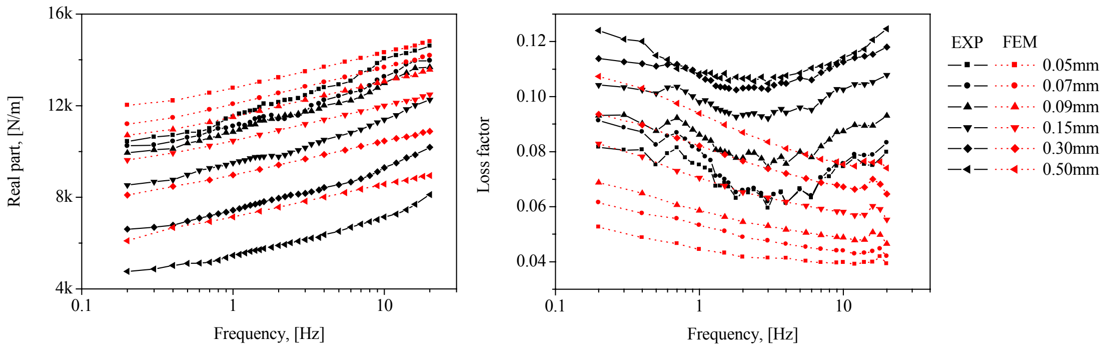

Figure.10 Comparison between measured- and calculated- complex stiffness of inflated diaphragm k_d^*; real part : $Re[k_d^*]$, loss factor : $Im[k_d^*]/Re[k_d^*]$

The calculation results using FE codes were represented by dotted lines in Figure 10. In the case of real part, those results of experiments and calculations exhibit qualitatively well matching characteristics for frequency- and dynamic amplitude-dependent behaviors(The discrepancies are from 3~15%). But it is not the case for loss factor showing a maximum discrepancy of 40%. Practically, it is extremely difficult to obtain a good prediction quality for the loss factor of viscoelastic materials, which seems to apply also our case. In addition, based on simple analysis for pneumatic spring, a fact was known that the stiffness of diaphragm rather than loss factor diminishes the improvement of vibration isolation performance of pneumatic spring. That is, more concentrations on the real part of complex stiffness are needed in evaluating the quality of calculations with FE codes. By referring again to results of real part in Figure 10, calculation method proposed in this paper can be validated. Furthermore, major portion of the indirectly measured results can be believed as the complex stiffness of the diaphragm.

CONCLUSIONS

This paper discussed how to compute the complex stiffness of inflated diaphragm by commercial FE codes, in which two stages of both nonlinear static- and linear dynamic- FE analysis were employed. The calculated results were compared with the indirectly measured ones obtained just by subtraction of the stiffness of the air in chamber from the measured complex stiffness of the pneumatic spring. Good matching for real part of complex stiffness, which are primary important in the improvement of vibration isolation performance in pneumatic spring, was achieved. Thus, it is concluded that calculation method proposed in this paper can be reasonably accepted for the calculation and/or prediction of diaphragm complex stiffness. Finally, the proposed method for calculation of the diaphragm complex stiffness can be usefully employed in the stage of design improvement of pneumatic spring.

REFERENCES

[1] C. G. Gordon. (1991) Generic criteria for vibration-sensitive equipment. *Proceedings of SPIE, San Jose, CA.*

[2] H. Amick, M. Gendreau and C. G. Gordon. (2002) Facility Vibration Issues for Nanotechnology Research. *Proceedings of the Symposium on Nano Device Technology, Hsinchu, Taiwan.*

[3] C. M. Harris and C. E. Crede (1961) Shock and Vibration Handbook. *McGraw-Hill.*

[4] D. B. DeBra (1984) Design of laminar flow restrictors for damping pneumatic vibration isolators. *CIRP Annals* 33(1), 351-356.

[5] C. Erin, B. Wilson and J. Zapfe (1998) An improved model of a pneumatic vibration isolator: Theory and experiment. *Journal of Sound and Vibration* 218(1), 81-101.

[6] J.H. Lee and K.J. Kim (2005) Complex stiffness of diaphragm in pneumatic springs for vibration isolation tables. *Proceedings of 11th Asia Pacific Vibration Conference, Langkawi, Malaysia.*

[7] ABAQUS Theory Manual(1997) *Hibbitt, Karlsson & Sorensen, Inc.*

[8] A. D. Nashif, D. I. G. Jones and J. P. Henderson (1986) Vibration damping. *New York: John Wiley & Sons, Inc.*

[9] Y.H. Shin, H.J. Lee and K.J Kim(2005) Consideration of static-strain-dependent dynamic complex modulus in dynamic stiffness calculation of mount/bushing by commercial finite element codes. *SAE 05NVC-61*

ACKNOWLEDGMENTS

This work has been financially supported by the Center for Nanoscale Mechatronics and Manufacturing of KIMM (Korea Institute of Machinery and Materials).